Supplementary Information

Covalent Docking of Large Libraries for the Discovery of Chemical Probes

Nir London[1,*], Rand M. Miller[2,*], Shyam Krishnan[3,*], Kenji Uchida[3], John J. Irwin[4], Oliv Eidam[1], Lucie Gibold[5,6,7], Peter Cimermančič[3], Richard Bonnet[5,6,7], Brian K. Shoichet[1,4,§], Jack Taunton[3,§]

[1] Department of Pharmaceutical Chemistry, University of California, San Francisco, San Francisco, CA 94158, USA
[2] Chemistry and Chemical Biology Graduate Program, University of California, San Francisco, San Francisco, CA 94158, USA
[3] Department of Cellular and Molecular Pharmacology, Howard Hughes Medical Institute, University of California, San Francisco, San Francisco, CA 94158, USA
[4] Faculty of Pharmacy, Donnelly Centre, 160 College St. Room 604, University of Toronto, Toronto, Canada M5S 3E1.
[5] Clermont Université, UMR 1071 Inserm/Université d'Auvergne, 63000 Clermont-Ferrand, France
[6] INRA, USC 2018, 63000 Clermont-Ferrand, France
[7] Service de Bactériologie, Centre Hospitalier Universitaire, 63000 Clermont-Ferrand, France

[*] Equal contribution
[§] Corresponding authors: bshoichet@gmail.com (for correspondence relating to the docking method and to covalent inhibition of β-lactamase); jack.taunton@ucsf.edu (for correspondence relating to covalent inhibition of kinases)

Supplementary Results

Supplementary Tables

Supplementary Table 1. Characterization of commercially available and virtual electrophile libraries

Electrophile	Subset[a]	N[b]	HA[c]	Rot.[d]	MW[e]	AlogP[f]	Acc.[g]	Don.[h]	SMARTS
Boronic acid		22,683	20±7.1	4.3±2.5	283±98.3	3.3±1.5	3.9±1.4	1.8±1.1	OBO
α-ketoamide		13,674	26.5±3.9	5.5±1.7	365.5±52.7	2.8±1.2	3.8±1.2	1.2±0.8	O=[CR0]([#6])[CR0](=O)N[#6]
α,β-unsaturated carbonyl	Lead	230,997	21.8±2.4	4.4±1.6	307.8±30.9	2.2±1.1	3.7±1.4	1.0±0.8	C=CC=O[i]
	Frag.	27,175	15.4±2.4	2.8±1.4	216.5±30.8	1.4±1.3	2.9±1.2	0.7±0.8	
Carbamate	Lead	76,880	21.8±2.4	5.2±1.3	310.2±31	1.5±1.1	4.1±1	1.4±0.9	NC(=O)O
	Frag.	10,468	15.3±2	3.3±1.2	219±26.4	1±1.2	3.2±1	1.1±0.8	
Aldehyde	Lead	21,897	20.4±3.6	4.8±1.7	288.4±44.7	2.2±1.1	3.6±1.3	0.7±0.8	[CX3H1](=O)[#6]
Alkyl halides	Lead	17,715	16.6±3.5	3.7±1.7	275.2±43.3	2.2±1	2.6±1.4	0.7±0.8	[Br,Cl,I][CX4;CH,CH2] [j]
Epoxide		8,306	22.5±7.9	4±3.1	317.4±108.5	2.3±1.7	3.9±1.9	0.6±0.9	C1CO1
Aldehyde based cyanoacryl-amides	Frag.	11,525	18.5±2.8	3.7±1.3	258.5±37.1	1.1±1.1	3.8±1.2	1.5±0.8	See Supp. Fig. 9
Suzuki based cyanoacryl-amides	Frag. now	225,868	24.6±2.2	4.2±1	337.5±29.2	1.9±1	4.4±1.1	1.7±0.7	See Supp. Fig. 11

[a] Subset of ZINC [1] used as an additional filter:
Lead-like: 250 < molecular weight < 350; xLogP ≤ 3.5; rotatable bonds ≤ 7
Fragments: molecular weight < 250; xLogP ≤ 3.5; rotatable bonds ≤ 5
Fragments-now: same as fragments, limited to 'in-stock' compounds.
[b] Number of molecules in the library
Average (± standard deviation): [c] number of heavy atoms; [d] number of rotatable bonds; [e] molecular weight; [f] calculated logP (as implemented in Pipeline Pilot[2])
[g] number of hydrogen bond acceptors; [h] number of hydrogen bond donors.
[i] Note that this expression might capture less reactive moieties such as β-disubstituted enones.
[j] We did not include fluorine as most alkyl fluorides are non-reactive. Note however that fluoromethylketones are also excluded by this SMARTS pattern.

Supplementary Table 2. Comparison of covalent modeling of β-lactams with other docking software.

	DOCKovalent	CovalentDock	AutoDock	GOLD
Median (Å)[a]	2.36[b]			
Average (Å)[a]	2.87	3.4[c]	3.5[c]	4.0[c]

[a] The median/average Root Mean Square Deviation (RMSD) obtained by different covalent docking software over n=61 β -lactam adducts (Supplementary Table 3; [3]).
[b] The difference between the average and median performance is due to a few outliers with high RMSD values (Supplementary Table 3). A clear tendency was observed for high RMSDs for ligands with more than 11 rotatable bonds.
[c] Values are extracted from ref. [1] figure 10 for the top 1 prediction (as was used by DOCKovalent) note that these averages include 13 more non β-lactam structures.

Supplementary Table 3. β-lactam pose recapitulation benchmark*

PDB	#rot.[a]	RMSD (Å)	PDB	#rot.	RMSD (Å)	PDB	#rot.	RMSD (Å)
3BEB	6	2.12	2EX9	8	0.88	1FCO	11	3.43
1IYP[b]	7	1.94	1YMX	8	1.42	3N8S	11	2.21
2JBF	7	1.51	2ZC5	8	7.03	*3OCN*	12	1.73
2J8Y	7	0.96	3MZE	8	1.65	1BT5	12	4.93
1GHM	7	0.96	*3ITA*	8	2.69	3MZF	12	2.13
3LY4	7	2.27	2ZC3	8	2.36	3PBO	12	4.49
1GHP	7	2.40	1FCN	8	2.66	2ZQD	12	4.59
2ZD8	7	1.22	1B12	8	1.63	1PWD	12	2.36
1IYQ	7	1.56	3OCL	9	2.78	*2Z2M*	12	1.86
2EX8	7	0.96	2ZQA	9	1.66	3M6H	12	7.85
3MZD	7	4.60	2ZC6	9	1.33	1LL5	12	5.15
2ZQ9	7	3.23	*2ZC4*	9	1.24	3M6B	12	6.74
2EXA	7	2.56	1CEF	9	3.57	3IQA	12	4.70
1KVM	7	2.15	1LLB	9	6.03	2VGJ	13	4.25
1W8Y	7	3.49	*1LL9*	9	1.18	2ZQC	13	1.90
1CEG	7	1.04	3DWZ	9	2.11	1FR6	13	6.44
1FCM	7	2.46	*2C5W*	9	2.69	1PW8	14	3.57
1QMF	8	2.68	2XD1	10	3.97	1PWG	15	4.07
3A3I	8	1.99	3A3F	10	3.32	2EXB	17	3.88
2EX6	8	1.38	3A3E	10	1.81			
2WKH	8	1.66	1I5Q	11	3.71			

[a] Number of rotatable bonds in the covalent adduct.
[b] PDBs in italics indicate cases where different protonation states were available. The lower RMSD is reported in these cases.
* Note that the original benchmark reported in [3] contained two additional cases 3BEC and 3KGO, however these had non-realistic covalent bond angles and were excluded from the analysis.

Supplementary Table 4. DOCKovalent retrospective virtual screen performance

Target	PDB	Electrophile	Type[a]	Lib. Size[b]	Ligands[b]	AUC[d]	logAUC[e]
EGFR	4G5J	α,β-unsaturated carbonyl	Product	215,000[c]	50	85.2	27.5
FAAH	3LJ7	Boronic Acid	Product	11,000	142	84.3	25.1
		Carbamate	HEI	71,000[c]	61	77.8	13.5
AChE	4EY6	Carbamate	HEI	72,000[c]	232	74.8	17.0
NS3	1RTL	α-Ketoamide	HEI	13,500	93	16.5	-10.7

[a] Covalent ligands were docked either in their product form, or in their High Energy Intermediate (HEI) form (Supplementary Fig. 1).
[b] We report the number of molecules (both ligands and decoys) for which a non-clashing pose was found. E.g. for EGFR poses were found for 50 known inhibitors and 215,000 decoys containing an α,β-unsaturated carbonyl group.
[c] ZINC was filtered for molecules containing the electrophiles. To limit the docking library size for the α/β-unsaturated carbonyl and carbamate libraries we included only lead-like molecules (250 ≤ molecular weight ≤ 350 ; xLogP ≤ 3.5 ; Number of rotatable bonds ≤ 7).
[d] Area Under ROC curve (AUC). 100% corresponds to perfect ranking. 50% corresponds to random ranking.
[e] Adjusted logAUC is a measure for early enrichment [4], and random ranking corresponds to a logAUC of 0.

Supplementary Table 5. RMSDs for AmpC/Boronic acid pose recapitulation benchmark

PDB	RMSD(Å)	PDB	RMSD(Å)	PDB	RMSD(Å)
1KDS	0.43	1MXO	1.11	4E3O	2.43
4E3M	0.62	2RCX	1.15	1IEM	3.05
4E3N	0.65	1C3B	1.19	1GA9	3.37
1MY8	0.67	3O86	1.72	1FSW	3.49
1KDW	0.69	4E3L	1.73	3BM6	3.53
4E3J	0.74	3O88	1.93	3BLS	5.47[a]
1KE0	0.91	3O87	1.97	4LV0	0.46 [b]
4E3K	0.97	2I72	2.19	4E3I	6.66

[a] RMSD to previously deposited incorrect pose. See results section on MAPB.
[b] RMSD to newly deposited MAPB structure.

Supplementary Table 6. Specificity of new boronic acids for AmpC

K_i [μM][a]				
Compound	**2**	**3**	**5**	**7**
AmpC	0.18	0.04	0.6	0.01
Trypsin	>5mM	138	>5mM	1306
Elastase	248	3331	382	2882
α-CT	167	0.3	1010	99
Specificity[b]				
Trypsin	>27,777	3450	>8,333	130600
Elastase	1378	83275	637	288200
α-CT	928	8	1683	9900

[a] K_i is calculated based on single point measurement, based on literature K_m values of respective protease substrates (see Methods).

[b] specificity is calculated as K_i Protease/K_i AmpC.

Supplementary Table 7. Lack of activity of predicted AmpC non-binders

Compound	Dock Rank	K_i [μM]	Ligand Eff. [a]
14	10694	3.21[b]	0.43
15	10706	N/A[c]	N/A
16	10819	N/A	N/A
17	10835	N/A	N/A
18	10982	N/A	N/A

[a] Ligand efficiency based on the calculated K_i

[b] IC_{50} was calculated based on a full dose response curve (Supplementary Fig. 15)

[c] N/A: < 10% inhibition at 10 μM

Supplementary Table 8. Antibacterial activity of new AmpC inhibitors in the absence of cefotaxime

Strain [a]	MIC (μg/ml)			
	2	**3**	**5**	**7**
Citrobacter freundii	> 2048	> 2048	2048	2048
Enterobacter cloacae	> 2048	> 2048	1024	1024
Enterobacter aerogenes	> 2048	> 2048	2048	1024
Escherichia coli Hcase	> 2048	> 2048	1024	2048
Escherichia coli Hcase	> 2048	> 2048	1024	1024
Escherichia coli TEM3	> 2048	> 2048	1024	1024
Escherichia coli CTXM14	> 2048	> 2048	1024	2048

[a] clinical isolates previously shown to be resistant to third generation cephalosporins.

Supplementary Table 9. Docking ranks of Suzuki library combinations

		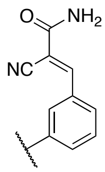		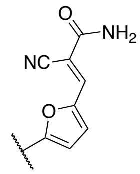		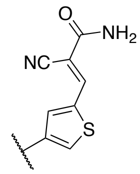		Rank with best linker[c]		
	# hits[a]	PDB[b]	Rank	PDB	Rank	PDB	Rank	PDB	Rank	Best linker
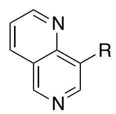	2	3lxl	636	3lxk	639	3lxk	948	3lxk	16	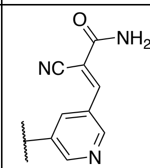
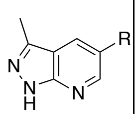	4	3lxk	425	4hvg	183	4hvg	5562	4hvg	183	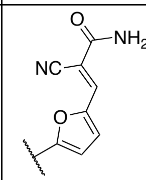
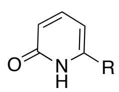	2	3lxl	525	4hvg	1406	4hvh	6906	4hvg	66	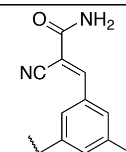
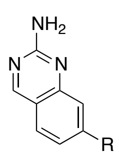	1[d]	3lxl	290	4hvg	5700	4hvg	3056	3lxl	290	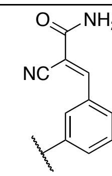
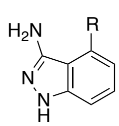	7	3pjc	1	4hvd	3	3lxl	10	3pjc	1	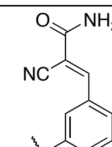
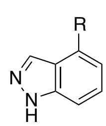	5	3pjc	121	3pjc	164	3pjc	488	4hvi	22	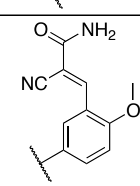
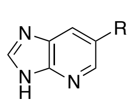	4	3pjc	1235	3pjc	2003	4hvg	98	3lxl	73	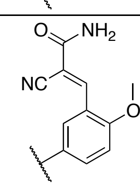
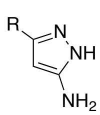	8	3lxl	505	3lxk	411	4hvg	149	3lxk	6	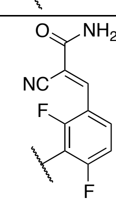

[a] Number of PDB templates for which this scaffold ranked with any linker in the top 500. [b] PDB template for which this combination of scaffold and linker scored best. [c] The best rank of this scaffold with any of the 50 boronic acid aldehyde linkers; the linker that achieved this rank is depicted in the right-most column. [d] The only candidate chosen using a native Cys909 rotamer (+60), all other compounds were selected based on docking to an alternative Cys rotamer (–60).

Supplementary Table 10. Data collection and refinement statistics

	AmpC/MAPB (4LV0)	AmpC/**3** (4LV1)	AmpC/**7** (4LV2)	AmpC/**14** (4LV3)	RSK2 T493M/**24** (4M8T)
Data collection					
Space group	C2	C2	C2	C2	$P4_12_12$
Cell dimensions					
a, *b*, *c* (Å)	118.46, 77.46, 97.51	118.58, 77.54, 97.64	117.67, 78.14, 97.25	117.67, 78.14, 97.25	46.99, 46.99 291.10
α, β, γ (°)	90, 116.04, 90	97.64 90, 116.46, 90	90, 116.28, 90	90, 115.72, 90	90, 90, 90
Resolution (Å)	50-1.65	50-1.74	50-1.65	50-1.42	46.38 – 3.0
R_{merge}	3.1 (51.9)	4.1 (53.1)	5.6 (75.3)	3.5 (42.1)	18.5 (20.9)
$I / \sigma I$	20.6 (2.1)	20.6 (2.4)	14.8 (2.1)	21.7 (3.5)	13.1 (6.0)
Completeness (%)	96.5 (94.1)	99.7 (99.8)	99.5 (96.9)	96.5 (93.9)	98.7 (99.9)
Redundancy	2.6 (2.5)	3.7 (3.7)	4.5 (4.15)	3.9 (3.6)	23.4 (26.1)
Refinement					
Resolution (Å)	45.67-1.65 (1.675 -1.65)	45.55-1.74 (1.769-1.74)	45.58-1.65 (1.673-1.65)	44.18-1.42 (1.436-1.42)	46.39 – 3.00 (3.78 – 3.00)
No. reflections	91645	81114	94599	144017	7265
R_{work} / R_{free}	16.4 (25.5) / 19.4 (29.7)	17.0 (25.4) / 19.5 (28.7)	17.2 (29.7) / 19.2 (29.8)	17.8 (23.9) / 19.2 (25.1)	25.3 (29.8) / 31.3 (38.0)
No. atoms					
Protein	5558	5542	5538	5507	2370
Ligand/ion	25	70	55	39	20
Water	802	495	428	699	0
B-factors					
Protein	20.8	19.9	23.6	25.2	59.5
Ligand/ion	20.3	21.2	29.6	26.5	55.3
Water	29.8	26.0	30.2	35.8	55.1
R.m.s. deviations					
Bond lengths (Å)	0.014	0.014	0.014	0.012	0.011
Bond angles (°)	1.51	1.5	1.48	1.46	0.91

* All datasets were collected from single crystals. The highest-resolution shell is shown in parentheses.

Supplementary Table 11. Experimental details for JAK3 kinase selectivity assays

Kinase	Vendor #	[enzyme] nM	[ATP] μM	Incubation (hours)
JAK1	Invitrogen-PV4774-877058D	0.5	70	2
JAK2	Invitrogen-PV4210-784633G	0.2	12	2
JAK3	Invitrogen-PV3855-1026644	0.5	2	2
TYK2	Invitrogen-PV4790-884908A	1.0	35	2
BLK	BPS-40401-111102	0.1	20	3
BMX	BPS-40402-110711	0.5	75	3
BTK	BPS-40405-130315-GC2	0.7	16	3
EGFR	BPS-40187-131015-G2	0.4	3	3
ERB-B2	BPS-40230-110913-5	2.0	50	3
ERB-B4	CARNA-08-118 -08CBS-0652	0.8	15	3
TEC	CARNA-08-182-10CBS-0017	1.0	50	3
ITK	CARNA-08-181-10CBS-1259	0.2	10	4
TXK	INVITROGEN-PV5860-750657B	0.5	100	3

Supplementary Figures

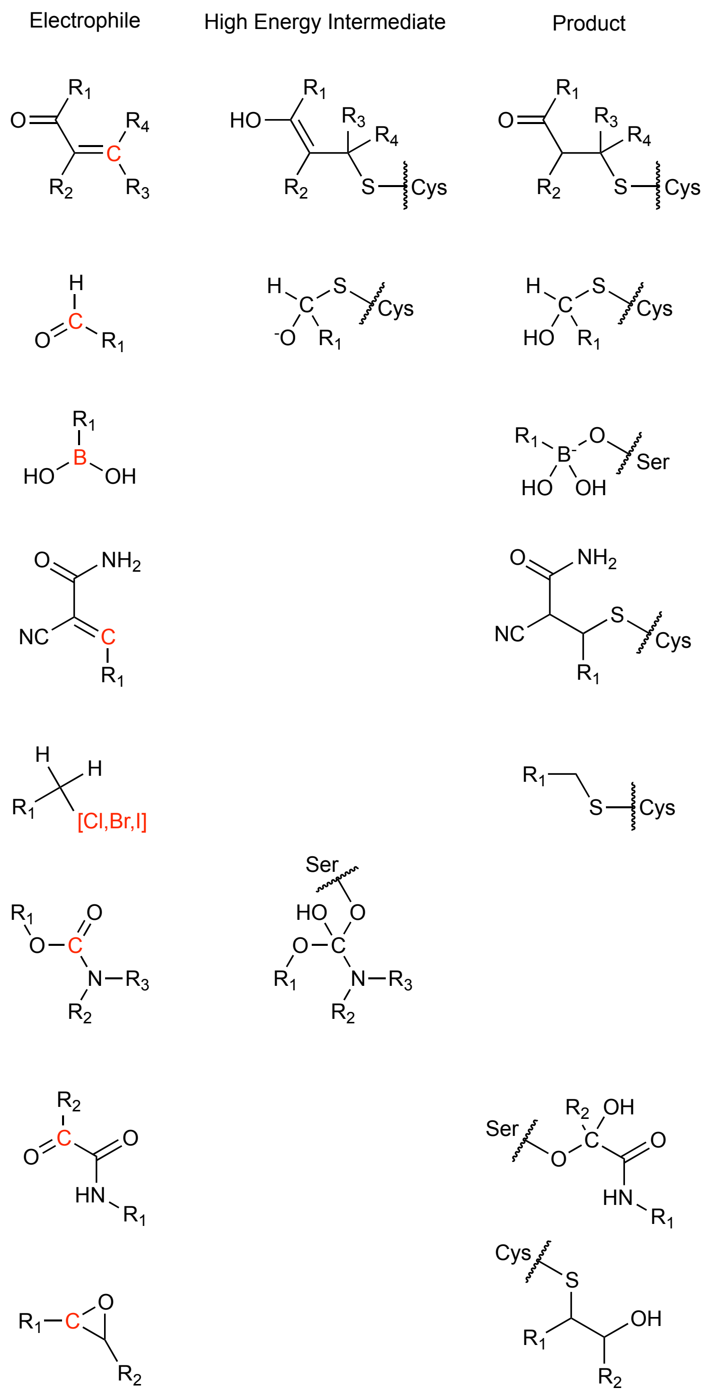

Supplementary Figure 1. Electrophiles used in this study.
Structures of electrophiles available for docking, from top to bottom: α,β-unsaturated carbonyl, aldehyde, boronic acid, cyanoacrylamide, alkyl halide, carbamate, α-ketoamide and epoxide. The electrophilic atom is indicated in red. The high-energy intermediate (center) or product (right) form for each electrophile is depicted as a covalent adduct to a protein nucleophile (cysteine or serine). Note that in some cases a new chiral center is formed upon reaction with the target nucleophile.

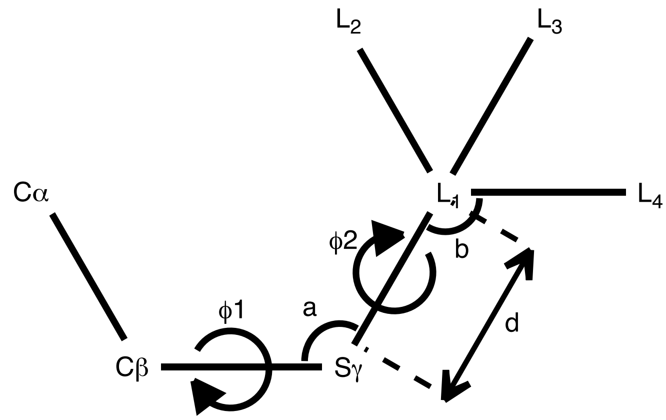

Supplementary Figure 2. Sampling parameters of DOCKovalent
Schematic of an electrophilic ligand (L_1-L_4) covalently attached to a Cys residue (for illustration). The dihedral angles ϕ1 (Cα-Cβ-Sγ-L_1) and ϕ2 (Cβ-Sγ-L_1-L_2) are exhaustively sampled in steps of 20°. The covalent bond length 'd' and bond angles 'a' (Cβ-Sγ-L_1) and 'b' (Cβ-Sγ-L_4) are set to user-specified ideal values, which are electrophile-specific and sampled within a range of these values (range and sampling steps are also user specified). See Methods section for the values used in this study.

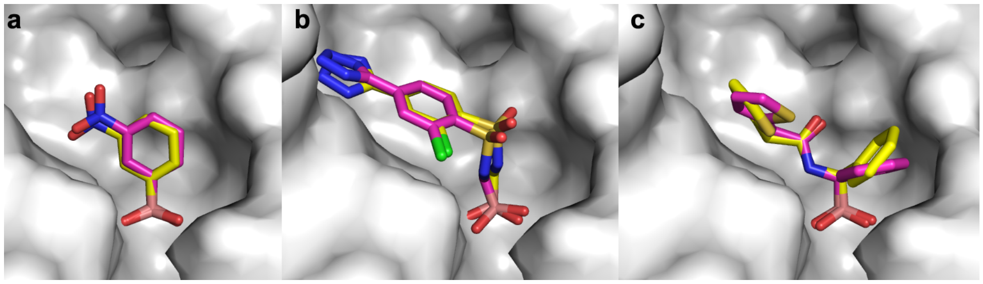

Supplementary Figure 3. Retrospective pose recapitulation of boronic acids binding to AmpC.

DOCKovalent pose predictions (magenta) of boronic acid binding to AmpC (white) closely match the crystal pose (yellow) of PDBs: **a.** 1KDS (0.43 Å) **b.** 4E3M (0.62 Å) **c.** 1MY8 (0.67 Å). See Supplementary Table 5 for RMSD values of the entire benchmark.

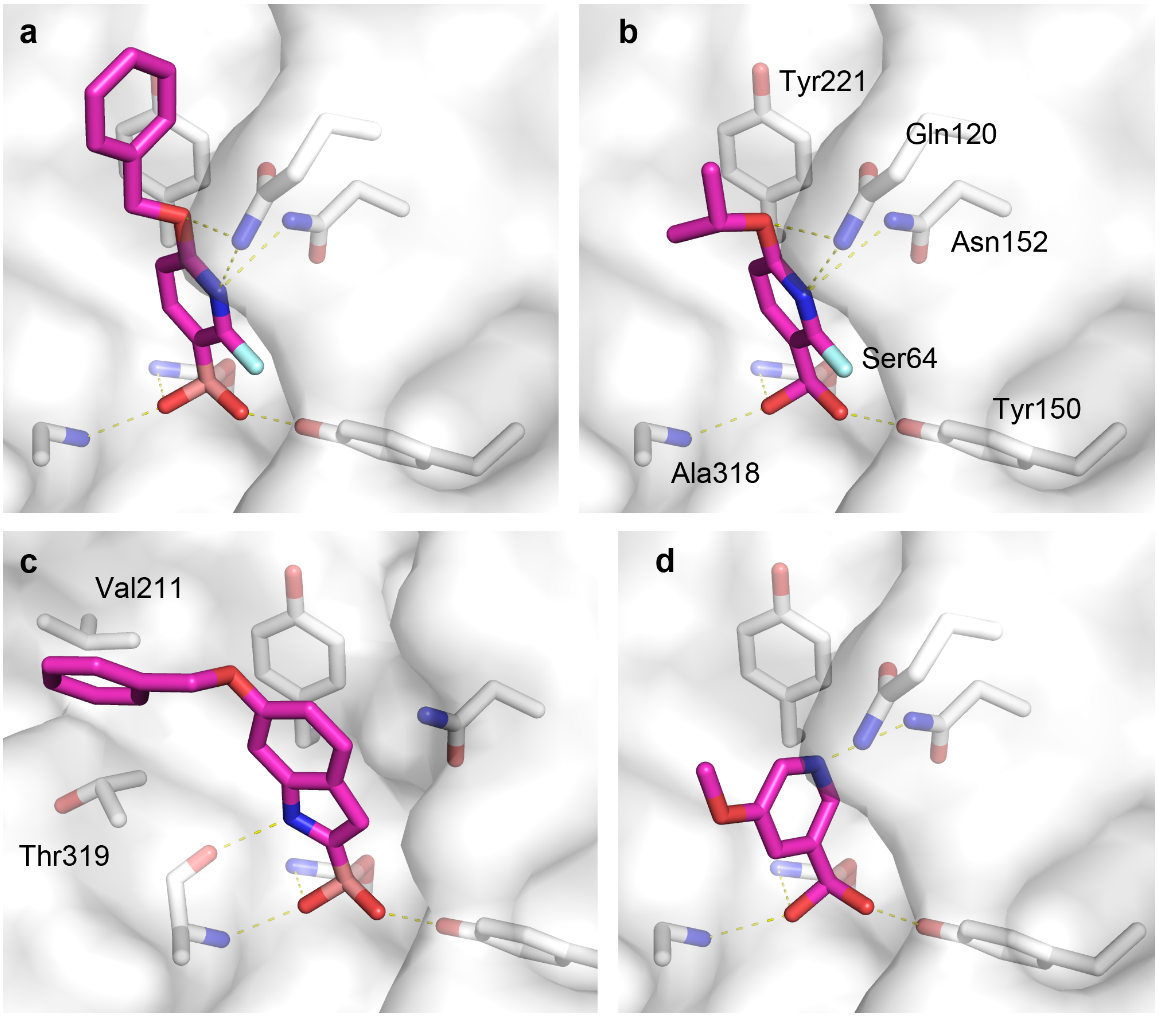

Supplementary Figure 4. Docking predictions of new boronic acid AmpC inhibitors.

All boronic acids docked to AmpC with a canonical binding mode, where the boronic acid occupies the oxyanion hole consisting of the backbone amides of Ala318 and Ser64, and accepts a hydrogen bond from Tyr150. **a,b.** Pyridyl boronic acids **2** and **5,** respectively, are predicted to hydrogen bond to Asn152 and Gln120 via the pyridine nitrogen and the ether oxygen. **c.** Indole boronic acid **4** is predicted to stack against Tyr221 and form a hydrogen bond with the backbone carbonyl of Ala318. The hydrophobic benzyl ether is predicted to project into a hydrophobic pocket created by Thr319 and Val211. **d.** Methoxypyridine **6**, which scored poorly in the docking run, was selected for testing because several high-ranking derivatives of this compound were not available for purchase. See Table 1 for the docking ranks, K_i and ligand efficiencies of these inhibitors.

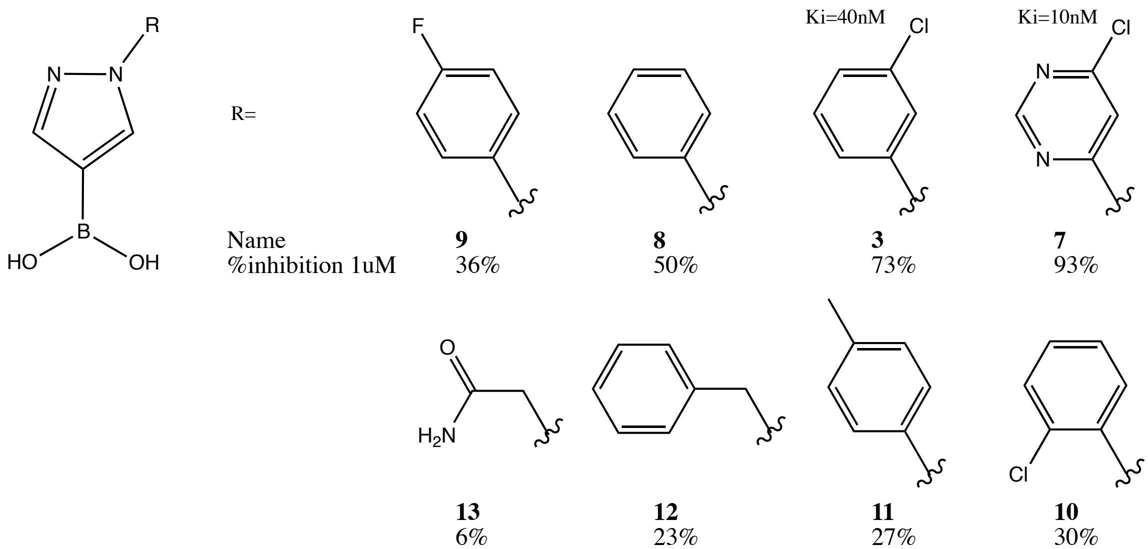

Supplementary Figure 5. AmpC inhibition by analogs of compound 3.
Structures of each boronic acid analog of **3,** and the percent inhibition of AmpC at 1 μM inhibitor. This SAR series shows a preference for substitution at the meta position of the phenyl or pyrimidine substituent.

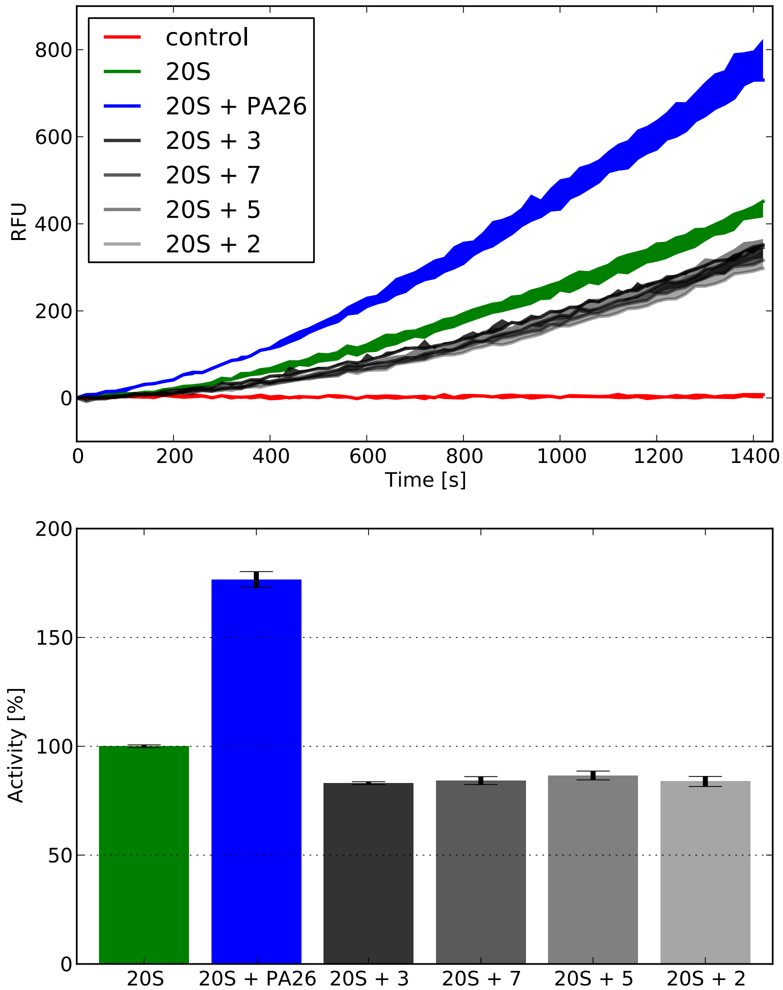

Supplementary Figure 6. New AmpC boronic acid inhibitors are selective against the yeast proteasome. a. Proteasome activity in the presence of compounds **2**,**3**,**5** and **7** at a concentration of 100 μM or the proteasome activator complex PA26 at a concentration of 5 nM was monitored over time **b.** The substrate hydrolysis rates do not show significant inhibition of the proteasome by the compounds. Rates were determined for the last 10 minutes of the experiment.

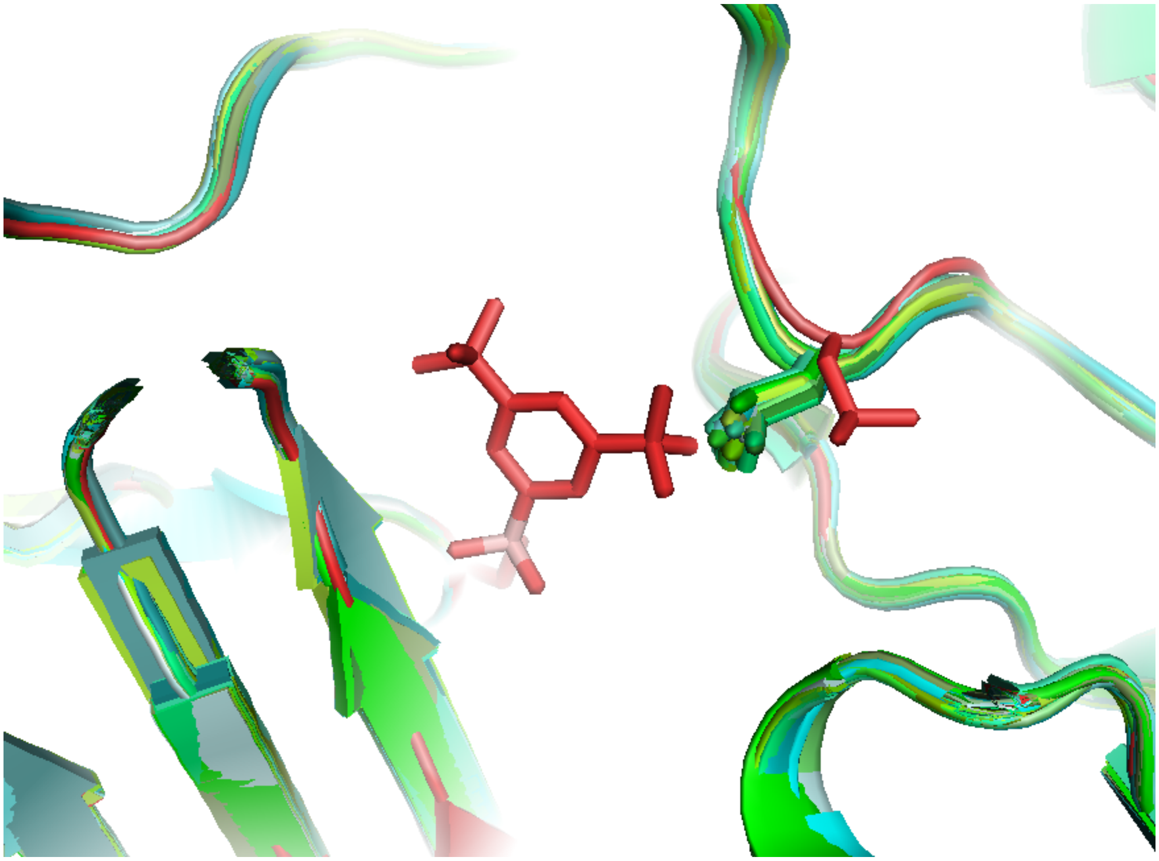

Supplementary Figure 7. AmpC adopts a unique conformation to bind compound 14.
Binding of compound **14** to AmpC (red) induces a unique conformation of loop 117-120, with Leu119 adopting a rotamer that is not observed in 23 published complex structures of AmpC with boronic acids (green).

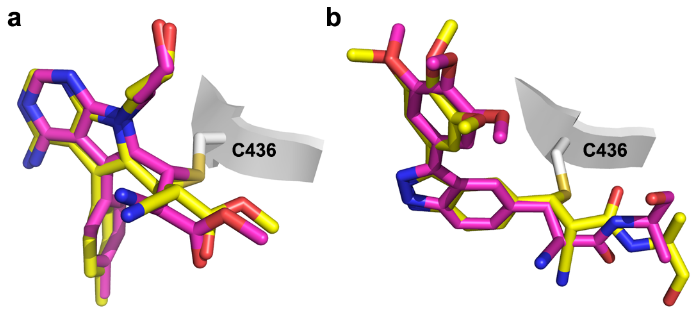

Supplementary Figure 8. Retrospective docking of cyanoacrylamides to RSK2. DOCKovalent predictions (magenta) accurately recapitulate the crystallographic poses (yellow) of cyanoacrylamide inhibitors of RSK2. **a.** Recapitulation of ligand binding in PDB: 4D9T with an RMSD of 0.66 Å overall (0.48 Å over the scaffold alone). **b.** Recapitulation of ligand binding in PDB: 4JG8 with an RMSD of 1.52 Å overall (0.91 Å for the scaffold alone).

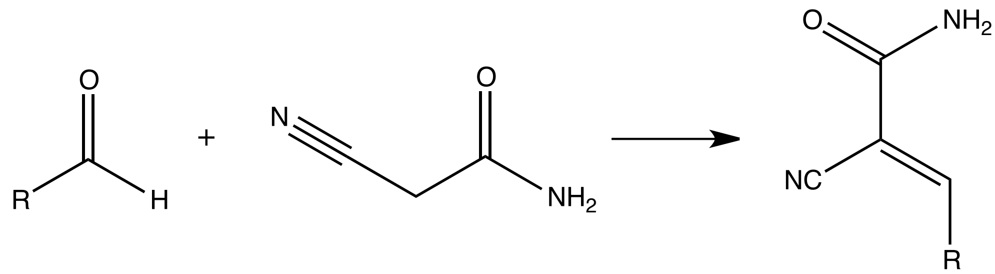

Supplementary Figure 9. Cyanoacrylamides can be synthesized from aldehydes by Knoevenagel condensation.

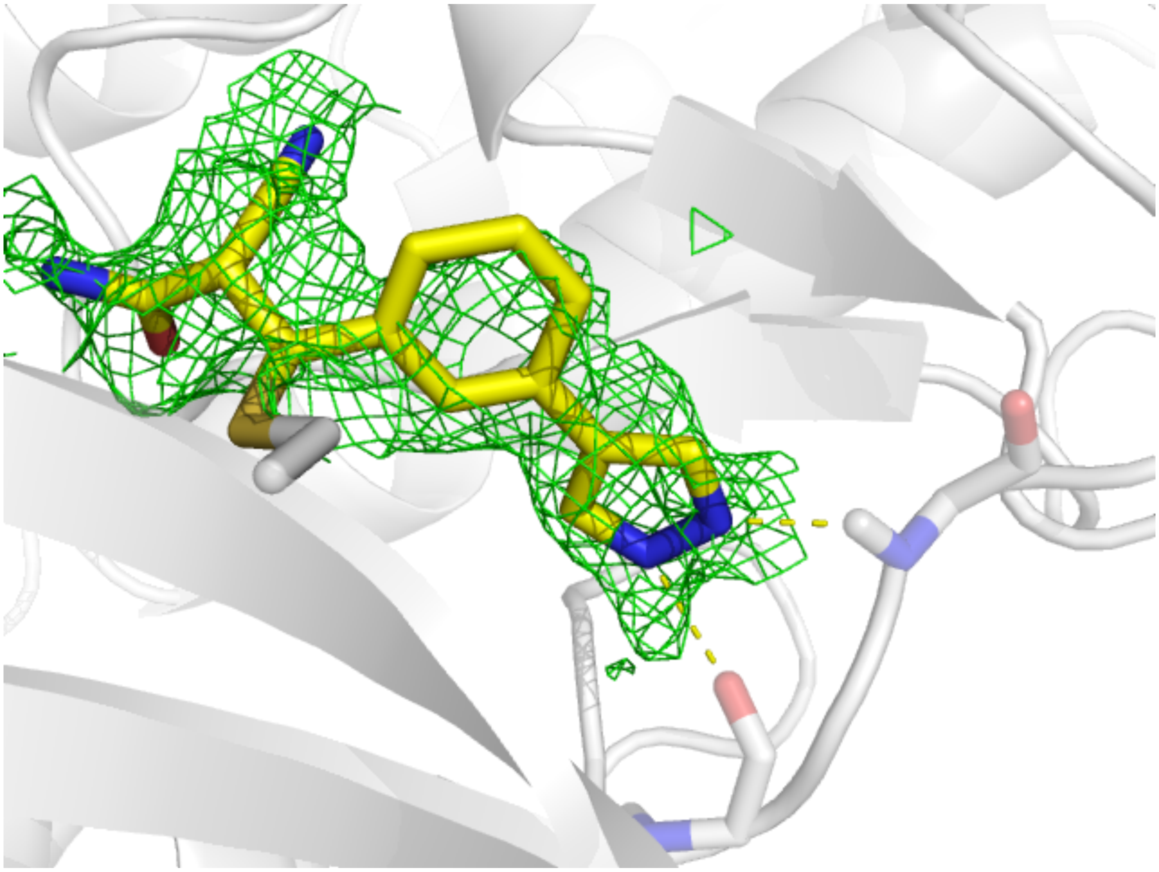

Supplementary Figure 10. Crystal structure of compound 24 covalently bound to T493M RSK2. The co-crystal structure of compound **24** (yellow) bound to T493M RSK2 (white) was determined at 3.0 Å resolution. Even at this modest resolution, the electron density (F_o-F_c omit map in green) allowed unambiguous modeling of the phenylpyrazole fragment and the covalent bond to Cys436.

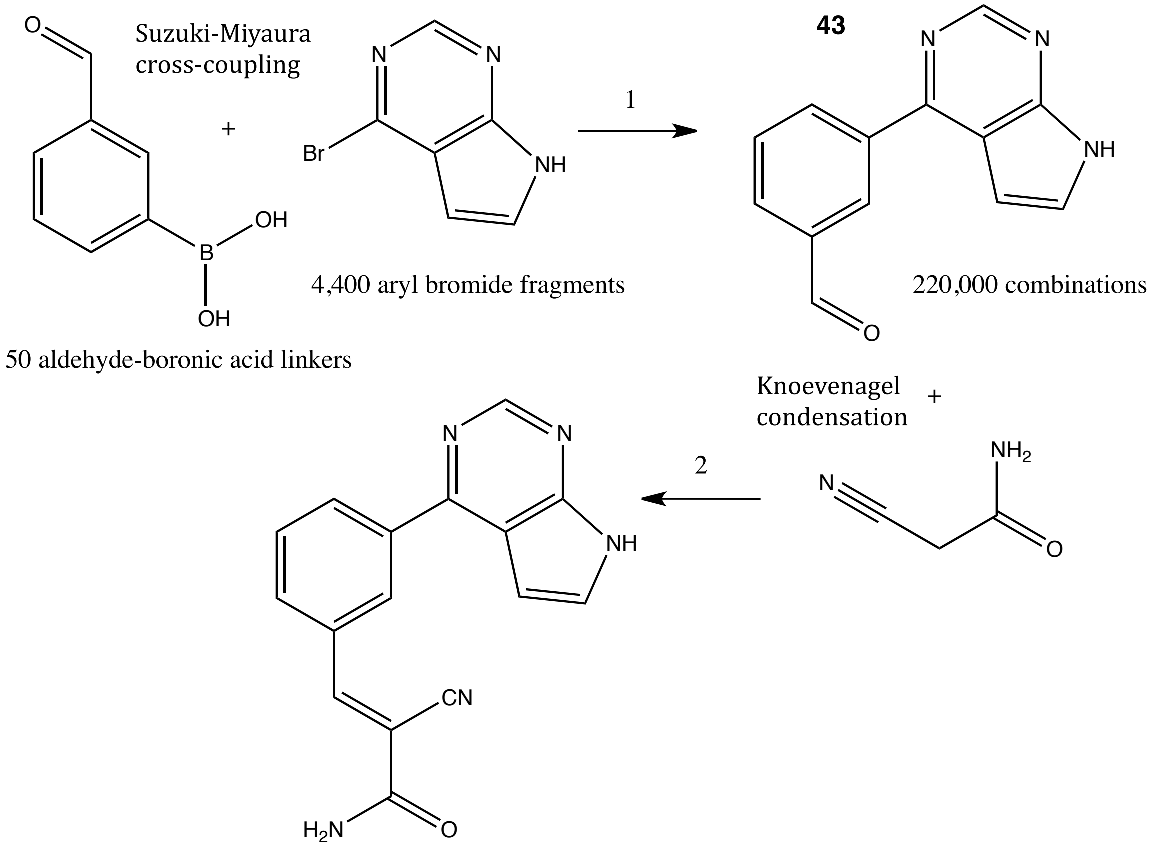

Supplementary Figure 11. A combinatorial library of cyanoacrylamides can be synthesized in two steps: 1. Suzuki-Miyaura cross-coupling of an aldehyde containing boronic acid followed by 2. Knoevenagel condensation to form the final cyanoacrylamide. This scheme is exemplified by fragments that can be used to synthesize compound **27**. The *in silico* virtual library based on this scheme combined 50 boronic acids with 4,397 aryl bromide fragments to form a final library of 219,850 cyanoacrylamides.

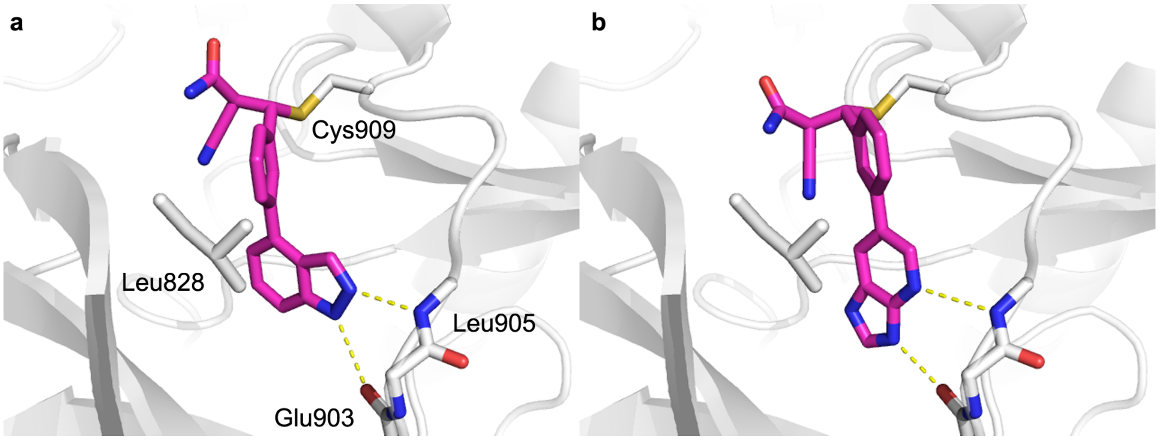

Supplementary Figure 12. Docking pose predictions for compounds 31 and 33 in complex with JAK3. a. compound **31** packs its meta-phenyl linker against Leu828, while placing an indazole moiety to form hydrogen bonds with the hinge backbones of Leu905 and Glu903 **b.** compound **33** forms the same hydrogen bonds to the hinge via an alternative placement of an imidazo[4,5-b]pyridine.

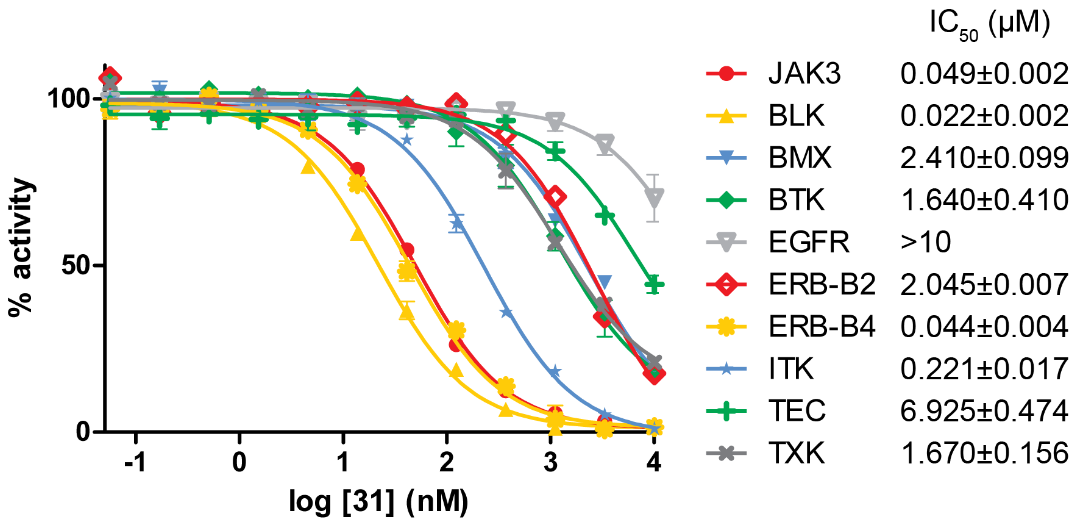

Supplementary Figure 13. Compound 31 is selective against most kinases that contain a cysteine equivalent to JAK3 Cys909. Dose-response curves for compound **31** against the nine additional human kinases containing an homologous cysteine to JAK3.

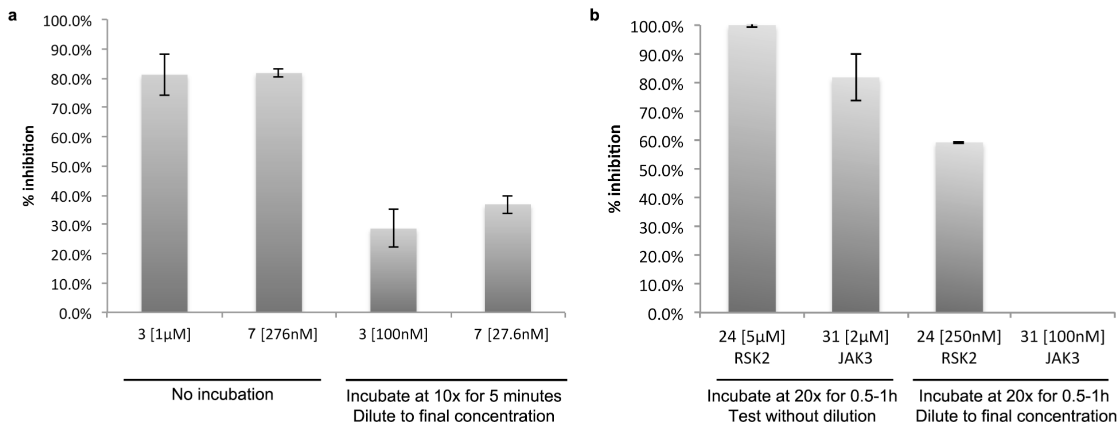

Supplementary Figure 14. Newly discovered covalent inhibitors are reversible. a. Compounds **3** and **7** were tested for inhibition at about 5 x IC_{50} concentration with no incubation time (starting the reaction by adding AmpC) and showed ~80% inhibition. When incubated at this concentration for 5 minutes and then diluted 10x the inhibition of ~30% reflected the new diluted concentration and not the high incubation concentration – indicating these compounds are rapidly reversible. **b.** Compounds **24** and **31** were incubated with RSK2 (0.5 hour) and JAK3 (1 hour) respectively at ~IC_{90} concentration. They were then diluted 20x into reaction buffers containing high ATP concentration (100 μM) and either the same concentration of the inhibitor (left columns) or no inhibitor (right columns). The partial retention of inhibition seen for **24** after dilution indicates that it has a relatively slow off-rate, as was previously reported for RSK2 cyanoacrylamide inhibitors. Nevertheless, both compounds are reversible.

Supplementary Figure 15. Raw images of cell-based autophosphorylation assays. Cropped gel images are shown in Figure 3.

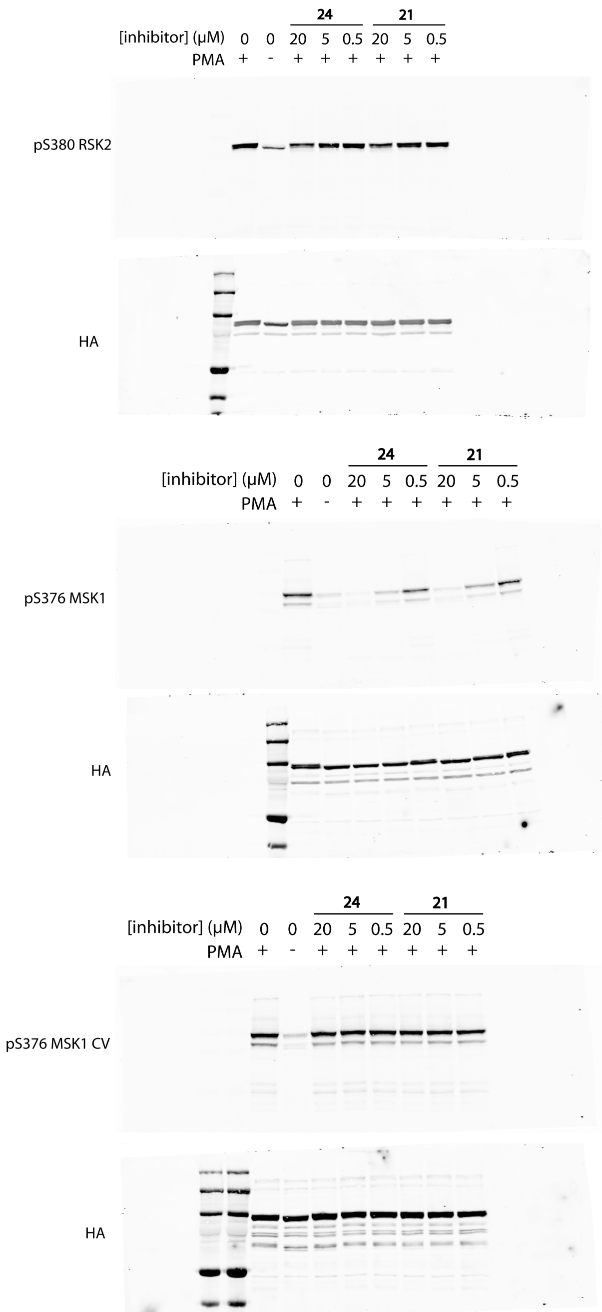

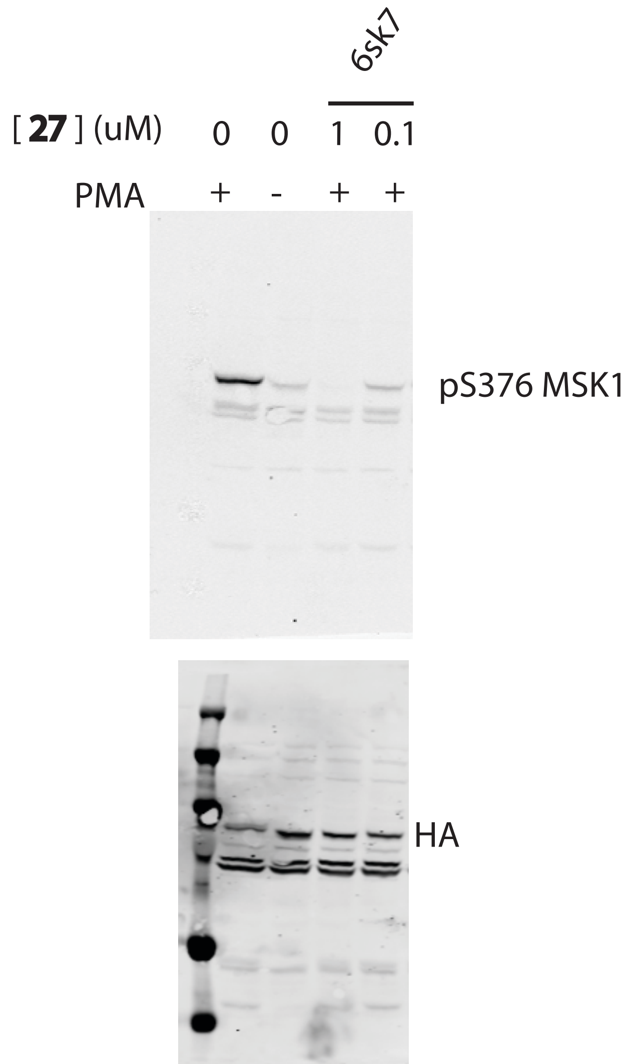

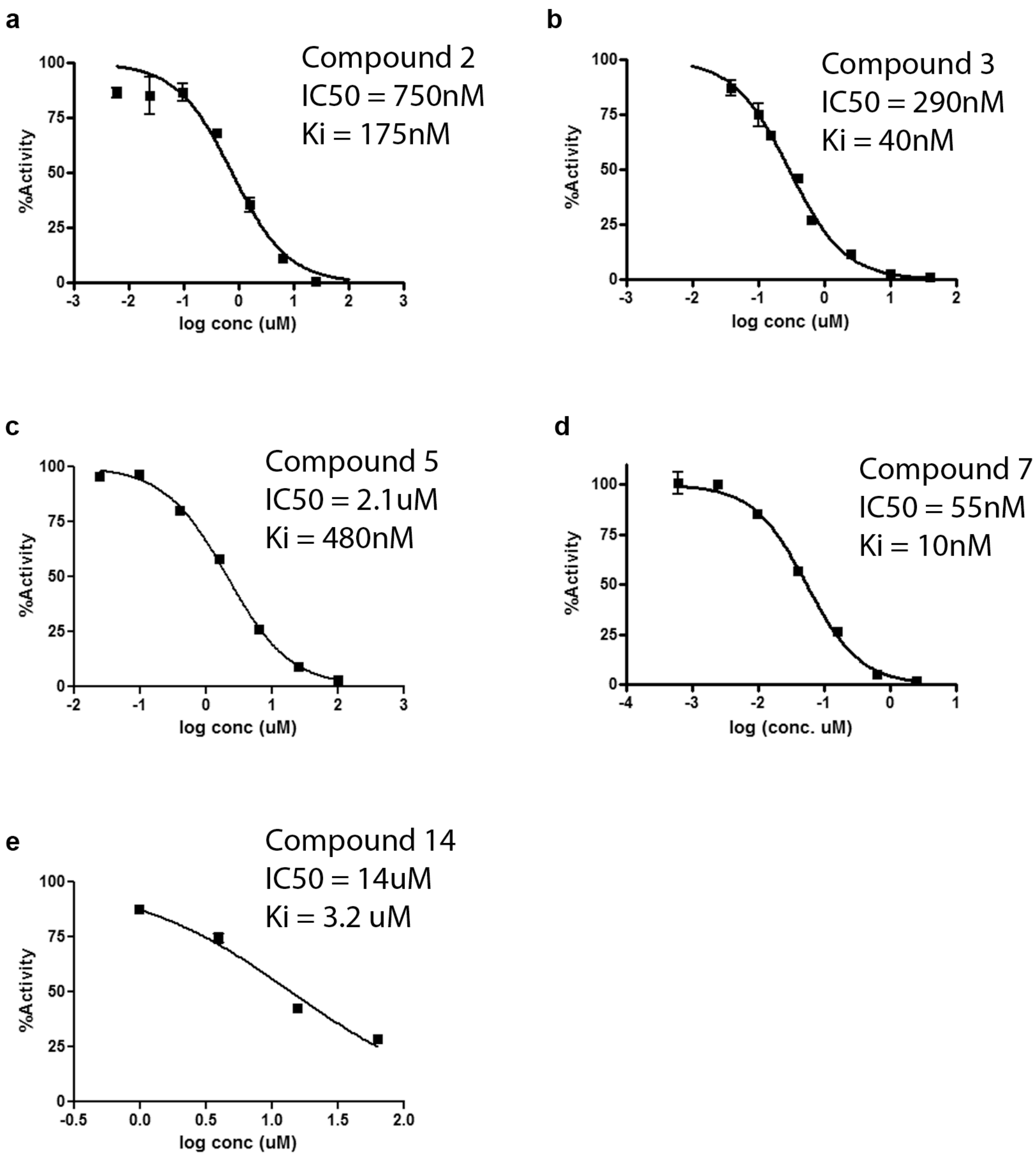

Supplementary Figure 16. IC_{50} curves for boronic acids 2, 3, 5, 7 and 14
IC_{50} values were determined by non-linear regression and K_i values were calculated using GraphPad software assuming competitive inhibition. The substrate (CENTA) concentration was 50 μM (in a,c-e.) or 100 μM (b). All Hill-slopes were approximately –1, indicating a 1:1 inhibitor stoichiometry.

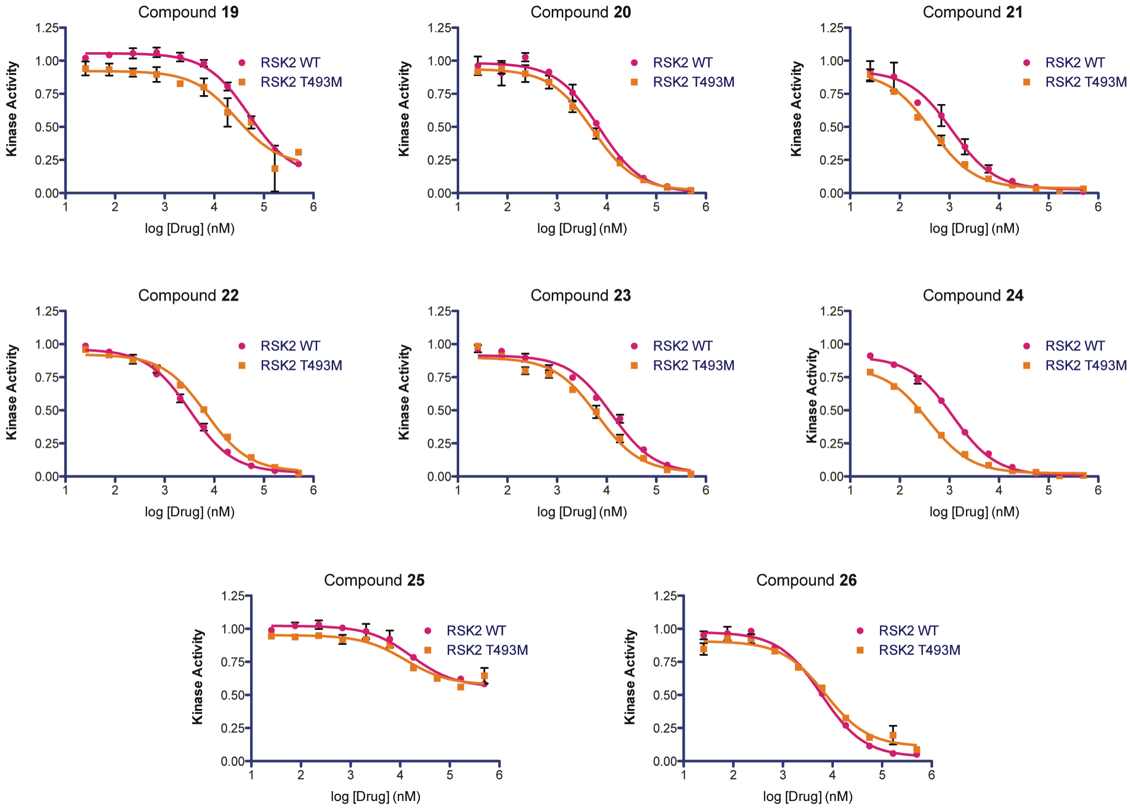

Supplementary Figure 17. IC_{50} curves for cyanoacrylamides 19 - 26
IC_{50} values were determined by non-linear regression using GraphPad software assuming competitive inhibition.

Supplementary Notes

Supplementary Note 1. Retrospective assessment of covalent docking. We tested method's ability to find known covalent ligands and geometries in retrospective calculations. In a pose recapitulation benchmark of 61 irreversibly bound β-lactams [3], the ligand structures predicted by DOCKovalent corresponded to the experimental structures with a median RMSD of 2.36 Å (Supplementary Tables 2,3), compared to an average 3.4 Å in the earlier study. This control calculation supports at least the ability of the method to recapitulate known geometries.

In addition to predicting geometries, a virtual screening method seeks to discover new ligands. A widely-used control for its ability to do so is to dock libraries composed of annotated ligands combined with decoy molecules that resemble the ligands but are not expected to bind. We therefore compiled libraries of known covalent inhibitors for each of the following five targets: epidermal growth factor receptor kinase (EGFR), fatty acid amide hydrolase (FAAH), acetylcholinesterase (AChE), and HCV protease NS3. The different inhibitors were driven by different electrophiles, including Michael acceptors, carbamates, boronic acids and α-ketoamides (Supplementary Table 4, Supplementary Fig. 1). To these libraries we added all purchasable molecules containing the same electrophiles to serve as decoys (Supplementary Table 4). While these "decoy" libraries likely contain genuine covalent inhibitors for these targets, we expected known binders to rank at the top of the hit list.

In four of the five covalent virtual screens, we observed substantial early enrichment of the annotated inhibitors versus the decoy molecules (area under the curve (AUC) of the Receiver Operating Characteristic (ROC) curve > 75%). Thus the adjusted logAUC, a metric that emphasizes early enrichment, was greater than 13.5; an adjusted logAUC of 0 corresponds to random ranking [4]. For NS3, the method performs poorly, likely due to the large number of rotatable bonds in known NS3 inhibitors, which on average had 17.3 rotatable bonds versus between 4.3 and 7.1 rotatable bonds for inhibitors of the other targets.

Supplementary Note 2. Synthetic Chemistry. All purchased chemicals were used as received without further purification. Solvents were dried by passage through columns (either alumina or activated molecular sieves) on a Glass Contour solvent system. NMR spectra were obtained on a Varian Inova 400 MHz spectrometer and referenced to the residual solvent peak. LC-MS analysis was performed on a Waters Acquity LCT UPLC equipped with a TUV detector (monitored at 254 nm) and a Waters Acquity UPLC 1.7 μm C-18 column, eluting at 0.6 mL/min with a 2.5 or 5 minute water:MeCN (with 0.1% formic acid) gradient method.

3-(4-((1*H*-1,2,4-triazol-1-yl)methyl)thiophen-2-yl)-2-cyanoacrylamide (**19**)
4-((1*H*-1,2,4-triazol-1-yl)methyl)thiophene-2-carbaldehyde (25 mg, 0.129 mmol) was dissolved in THF (0.5 mL) in a vial with a stirbar, to which was added 2-cyanoacetamide (11 mg, 0.129 mmol) and piperidine (12 μL, 0.129 mmol). The reaction was stirred for 7 hours. The precipitate was collected by filtration and dried *in vacuo* to afford cyanoacrylamide **19** (17 mg, 51%) as a tan solid. ^{1}H NMR (400 MHz, DMSO) δ 8.64 (s, 1H), 8.32 (s, 1H), 8.01 (s, 1H), 7.94 (s, 1H), 7.79 (br s, 1H), 7.74 (s, 1H), 7.69 (br s, 1H, overlaps peak at 7.74), 5.47 (s, 2H). ^{13}C NMR (125 MHz, DMSO) δ 162.52, 151.82, 144.18, 143.09, 137.99, 137.00, 136.31, 132.46, 116.46, 102.73, 46.93 LRMS. (ESI) Exact Mass: 259.05, Found: 260.3 (M + H^{+}).

Compounds **20**-**26** were synthesized analogously and purified by filtration or preparative TLC, eluting with hexanes/EtOAc. Yields refer to chromatographically and spectroscopically pure compounds.

4-(3-amino-2-cyano-3-oxoprop-1-en-1-yl)benzamide (**20**)
Yield: 47 mg (65%) ^{1}H NMR (400 MHz, DMSO) δ 8.22 (s, 1H), 8.12 (br s, 1H), 7.95 – 8.03 (m, 5H), 7.82 (br s, 1H), 7.56 (br s, 1H). ^{13}C NMR (125 MHz, DMSO) δ 167.0, 162.5, 149.7, 137.1, 134.4, 129.8, 128.2, 116.3, 108.2. LRMS (ESI) Exact Mass: 215.07, Found: 216.3 (M + H^{+}).

2-cyano-3-(3-(pyridin-4-yl)phenyl)acrylamide (**21**)
Yield: 33 mg (46%). ^{1}H NMR (400 MHz, DMSO) δ 8.69 (m, 2H), 8.34 (m, 1H), 8.31 (s, 1H), 8.05 - 8.60 (m, 2H), 7.96 (br s, 1H), 7.83 (br s, 1H), 7.70 – 7.76 (m, 3H). ^{13}C NMR (125 MHz, DMSO) δ 162.47, 150.44, 150.36, 145.98, 138.0, 132.88, 130.46, 130.16, 128.59, 121.25, 116.43, 107.65 (one carbon not observed). LRMS (ESI) Exact Mass: 249.09, Found: 250.2 (M + H^{+}).

3-(3-amino-2-cyano-3-oxoprop-1-en-1-yl)benzamide (**22**)
Yield: 36 mg (50%). ^{1}H NMR (400 MHz, DMSO) δ 8.37 (m, 1H), 8.23 (s, 1H), 8.09 (br s, 1H), 8.07 (s, 1H), 8.02 – 8.06 (m, 1H), 7.97 (br s, 1H), 7.81 (br s, 1H), 7.65 (t, 1H, *J* = 8Hz), 7.54 (br s, 1H). ^{13}C NMR (125 MHz, DMSO) δ 167.1, 162.6, 150.1, 135.3, 132.1, 132.0, 130.8, 129.7, 129.3, 116.2, 107.7. LRMS (ESI) Exact Mass: 215.07, Found: 216.3 (M + H^{+}).

2-cyano-3-(isoquinolin-6-yl)acrylamide (**23**)
Yield: 86 mg (60%). ^{1}H NMR (400 MHz, DMSO) δ 9.42 (s, 1H), 8.63 (d, 1H, *J* = 5.6 Hz), 8.62 (d, 1H, *J* = 1.6 Hz), 8.38 (s, 1H), 8.31 (dd, 1H, *J* = 1.6, 8.4 Hz), 8.14 (d, 1H, *J* = 8.4

Hz), 8.01 (br s, 1H), 7.91 (d, 1H, *J* = 5.6 Hz), 7.85 (br s, 1H). ^{13}C NMR (125 MHz, DMSO) δ 162.5, 153.4, 149.8, 145.0, 136.5, 131.7, 131.0, 129.3, 127.7, 127.6, 120.3, 116.4, 107.9. LRMS (ESI) Exact Mass: 223.07, Found: 224.3 (M + H$^+$).

<u>3-(3-(1*H*-pyrazol-4-yl)phenyl)-2-cyanoacrylamide (**24**)</u>
Yield: 44 mg (64%). ^{1}H NMR (400 MHz, DMSO) δ 8.23 (br s, 1H), 8.21 (s, 1H), 8.14 (m, 1H), 7.94 (br d, 2H), 7.78 – 7.83 (m, 3H), 7.55 (t, 1H, *J* = 8 Hz). ^{13}C NMR (125 MHz, DMSO) δ 162.62, 150.82, 136.13 (br), 133.86, 132.47, 129.70, 128.84, 127.11, 126.65, 125.63 (br), 120.19, 115.52, 106.78. LRMS (ESI) Exact Mass: 238.09, Found: 239.3 (M + H$^+$).

<u>2-cyano-3-(4-(2-fluorobenzoyl)-1-methyl-1*H*-pyrrol-2-yl)acrylamide (**25**)</u>
Yield: 42 mg (33%). ^{1}H NMR (400 MHz, DMSO) δ 8.00 (s, 1H), 7.89 (br s, 1H), 7.83 (s, 1H), 7.69 (d, 1H, *J* = 2 Hz), 7.54 - 7.67 (m, 3H), 7.32 – 7.40 (m, 2H), 3.83 (s, 3H). ^{13}C NMR (125 MHz, DMSO) δ 185.41, 162.92, 158.81 (*J* = 247 Hz), 136.64, 135.38, 132.88 (*J* = 8.4 Hz), 129.74 (*J* = 2.8 Hz), 128.30, 127.702 (*J* = 15.3 Hz), 125.35, 124.66 (*J* = 3.2 Hz), 117.11, 116.28 (*J* = 25 Hz), 115.37, 100.99, 34.53. LRMS (ESI) Exact Mass: 297.09, Found: 298.3 (M + H$^+$).

<u>2-cyano-3-(1,3-dimethyl-2-oxo-2,3-dihydro-1*H*-benzo[*d*]imidazol-5-yl)acrylamide (**26**)</u>
Yield: 19 mg (57%). ^{1}H NMR (400 MHz, DMSO) δ 8.19 (s, 1H), 7.80 (br s, 1H, overlaps peak at 7.77), 7.77 (s, 1H), 7.74 (d, 1H, *J* = 8 Hz), 7.67 (br s, 1H), 7.34 (d, *J* = 8 Hz), 3.38 (s, 3H), 3.35 (s, 3H). ^{13}C NMR (125 MHz, DMSO) δ 162.52, 153.39, 149.78, 145.02, 136.45, 131.67, 130.99, 129.30, 127.73, 127.66, 120.32, 116.34, 107.88. LRMS (ESI) Exact Mass: 256.10, Found: 257.3 (M + H$^+$).

<u>(*E*)-3-(3-(7*H*-pyrrolo[2,3-*d*]pyrimidin-4-yl)phenyl)-2-cyanoacrylamide (**27**)</u>
4-chloro-7*H*-pyrrolo[2,3-*d*]pyrimidine (145.2 mg, 0.945 mmol), 3-formylboronic acid (283.5 mg, 2.0 equiv.), *bis*-diphenylphosphanylferrocenepalladium(II) dichloromethane adduct (55 mg, 7 mol%) and potassium carbonate (261 mg, 2.0 equiv.) were suspended in dioxane/water (4:1 v/v, 5 mL). The mixture was degassed and heated to 110 ºC for 3 hours. The reaction mixture was then cooled, diluted with EtOAc (50 mL), and filtered through a pad of silica gel with EtOAc washes (20 mL). The filtrate and washes were combined and concentrated. The residue afforded was purified by silica gel chromatography (15:85 → 50:50 → 40:60 Hexanes: EtOAc) to afford 3-(7*H*-pyrrolo[2,3-*d*]pyrimidin-4-yl)benzaldehyde (79 mg, 38% yield, **43**) as a white solid. ^{1}H NMR (400 MHz, CD_3OD): 10.14 (s, 1H), 8.84 (s, 1H), 8.62 (s, 1H), 8.41 (d, *J* = 7.8 Hz, 1H), 8.10 (d, *J* = 7.7 Hz, 1H), 7.80 (t, *J* = 7.6 Hz, 1H), 7.59 (d, *J* = 3.5 Hz, 1H), 6.91 (d, *J* = 3.5 Hz, 1H); ^{13}C NMR (100 MHz, DMSO-d6): 193.6, 154.1, 152.8, 150.9, 140.1, 138.8, 136.7, 135.5, 134.2, 131.0, 129.9, 128.3, 114.6, 99.6; ESI-MS: 224.14 (MH$^+$).
3-(7*H*-pyrrolo[2,3-*d*]pyrimidin-4-yl)benzaldehyde (22.5 mg, 101 μmol), cyanoacetamide (12.7 mg, 1.5 equiv.) and piperidine•AcOH (2.9 mg, 0.2 equiv.) were suspended in EtOH (3 mL). The reaction mixture was heated at 60 ºC for 3 hours and then cooled in an ice bath to precipitate the cyanoacrylamide, which was filtered and dried, affording 27 mg (92% yield) of cyanoacrylamide **27** as a white solid. ^{1}H NMR (400 MHz, DMSO-d6): 8.88 (s, 1H), 8.72 (s, 1H), 8.39 (d, *J* = 7.8Hz, 1H),

8.36 (s, 1H), 8.08 (d, J = 7.7Hz, 1H), 7.98 (bs, 1H), 7.79 (m, 2H), 7.72 (m, 1H), 7.04 (m, 1H); ^{13}C NMR (100 MHz, DMSO-d6): 162.7, 154.2, 152.7, 150.9, 150.3, 138.8, 132.6, 132.1, 131.4, 129.9, 129.6, 128.2, 116.4, 114.5, 107.5, 99.8; ESI-MS: 290.3 (MH$^+$).

Cyanoacrylamides **28-42** were synthesized by analogous procedures and isolated by precipitation, or where necessary, purified by silica gel chromatography.

(E)-3-[3-(3-amino-1H-indazol-4-yl)phenyl]-2-cyanoacrylamide (**28**)
Yield: 0.8 mg (10% over 2 steps). ^{1}H NMR (400 MHz, DMSO-d6): 11.83 (s, 1H), 8.27 (s, 1H), 8.02 (m, 2H), 7.94 (bs, 1H), 7.79 (bs, 1H), 7.69 (m, 2H), 7.33 (m, 2H), 6.86 (m, 1H), 4.28 (s, 2H); ^{13}C NMR (100 MHz, DMSO-d6): 162.7, 150.5, 147.8, 142.2, 140.0, 134.5, 132.8, 132.1, 130.5, 129.3, 129.0, 126.4, 119.5, 116.6, 110.4, 109.5, 107.1; ESI-MS: 304.2(MH$^+$).

(E)-3-[5-(3-amino-1H-indazol-4-yl)furan-2-yl]-2-cyanoacrylamide (**29**)
Yield: 26.7 mg (39% over 2 steps). ^{1}H NMR (400 MHz, DMSO-d6): 12.02 (bs, 1H), 8.06 (s, 1H), 7.81 (bs, 1H), 7.69 (bs, 1H), 7.54 (d, J = 3.6Hz, 1H), 7.42–7.33 (m, 4H), 4.93 (s, 2H); ^{13}C NMR (100 MHz, DMSO-d6): 162.6, 157.1, 148.1, 148.0, 142.5, 135.4, 126.0, 123.6, 122.3, 118.8, 116.7, 113.6, 111.6, 109.0, 100.4; ESI-MS: 294.15(MH$^+$).

(E)-3-[4-(3-amino-1H-indazol-4-yl)thiophen-2-yl]-2-cyanoacrylamide (**30**)
Yield: 3.3 mg (5% over 2 steps). ^{1}H NMR (400 MHz, DMSO-d6): 11.82 (s, 1H), 8.45 (s, 1H), 8.15 (s, 1H), 8.04 (s, 1H), 7.84 (bs, 1H), 7.72 (bs, 1H), 7.30 (m, 2H), 6.91 (dd, J = 6.1, 1.5 Hz), 4.49 (s, 2H); ^{13}C NMR (125 MHz, DMSO-d6): 162.5, 148.2, 143.8, 142.2, 140.6, 138.5, 135.8, 132.2, 128.8, 126.2, 119.5, 116.7, 110.6, 109.6, 102.4; ESI-MS: 310.12(MH$^+$).

3-(3-(1H-indazol-4-yl)phenyl)-2-cyanoacrylamide (**31**)
Yield: 65 mg (70%). ^{1}H NMR (400 MHz, DMSO) δ 8.33 (s, 1H), 8.32 - 8.27 (m, 2H), 8.00 - 7.93 (m, 3H), 7.81 (br s, 1H), 7.73 (dd, 1H, J = 7.8, 7.8 Hz), 7.61 (d, 1H, J = 8.4 Hz), 7.48 (dd, 1H, J = 7.0, 8.4 Hz), 7.30 (d, 1H, J = 7.2 Hz). ^{13}C NMR (125 MHz, DMSO) δ 162.66, 150.67, 140.50, 140.16, 132.66, 132.65, 132.53, 131.85, 129.96, 129.32, 129.25, 126.35, 120.78, 119.75, 116.52, 109.99, 107.26. LRMS (ESI) Exact Mass: 288.10, Found: 289.3 (M + H$^+$).

3-(5-(1H-indazol-4-yl)furan-2-yl)-2-cyanoacrylamide (**32**)
Yield: 11 mg (74%). ^{1}H NMR (400 MHz, DMSO) δ 8.76 (s, 1H), 8.07 (s, 1H), 7.75 (d, 1H, J = 7.2 Hz), 7.65 (d, 1H, J = 8.3 Hz), 7.59 (d, 1H, J = 3.8 Hz), 7.55 (d, 1H, J = 3.8 Hz), 7.51-7.45 (m, 1H); ^{13}C NMR (125 MHz, DMSO) δ 162.73, 157.38, 148.13, 140.50, 135.19, 133.36, 126.11, 124.70, 120.90, 118.24, 118.03, 116.94, 111.76, 111.72, 100.18; LRMS (ESI) Exact Mass: 278.08, Found: 279.2 (M + H$^+$).

3-(3-(3H-imidazo[4,5-b]pyridin-6-yl)phenyl)-2-cyanoacrylamide (**33**)
Yield: 29 mg (61%). ^{1}H NMR (400 MHz, DMSO) δ 8.75 (s, 0.45H), 8.69 (s, 0.55H), 8.54 (s, 0.45H), 8.50 (s, 0.55H), 8.39 (s, 0.55H), 8.34-8.30 (m, 2H), 8.22 (s, 0.45H), 8.03-7.93 (m, 3H), 7.81 (br s, 1H), 7.73-7.67 (m, 1H); ^{13}C NMR (125 MHz, DMSO) δ

162.89, 150.86, 145.35, 142.92, 139.20, 132.86, 131.09, 130.20, 129.77, 128.91, 128.78, 116.7, 107.43; LRMS (ESI) Exact Mass: 289.10, Found: 290.3 ($M + H^+$).

<u>3-(4-(3H-imidazo[4,5-b]pyridin-6-yl)thiophen-2-yl)-2-cyanoacrylamide (**34**)</u>
Yield: 37 mg (82%). ^{1}H NMR (400 MHz, DMSO) δ 8.83-8.73 (m, 1H), 8.55-8.46 (m, 2H), 8.43 (s, 1H), 8.37 (d, 1H, J = 1.5 Hz), 8.24 (s, 1H), 7.86 (br s, 1H), 7.75 (br s, 1H); ^{13}C NMR (125 MHz, DMSO) δ 163.15, 162.66, 145.30, 144.27, 143.79, 142.73, 142.47, 142.33, 140.75, 140.09, 139.12, 130.74, 136.74, 136.60, 136.57, 131.31, 129.59, 124.83, 124.59, 118.47, 116.71, 103.62, 102.61; LRMS (ESI) Exact Mass: 295.05, Found: 296.1 ($M + H^+$).

<u>2-cyano-3-(3-(3-methyl-1H-pyrazolo[3,4-*b*]pyridin-5-yl)phenyl)acrylamide (**35**)</u>
Yield: 50 mg (88%). ^{1}H NMR (400 MHz, DMSO) δ 8.84 (d, 1H, J = 2.2 Hz), 8.54 (d, 1H, J = 2.2 Hz), 8.32 (s, 1H), 8.31-8.26 (m, 1H), 8.03-7.96 (m, 2H), 7.95 (br s, 1H), 7.82 (br s, 1H), 7.70 (dd, 1H, J = 7.8, 7.8 Hz), 2.55 (s, 3H); ^{13}C NMR (125 MHz, DMSO) δ 162.59, 152.07, 150.74, 147.66, 141.65, 138.92, 132.76, 130.66, 129.99, 129.03, 128.06, 127.50, 127.39, 116.55, 114.14, 107.31, 12.23; LRMS (ESI) Exact Mass: 303.11, Found: 304.1 ($M + H^+$).

<u>2-cyano-3-(5-(3-methyl-1H-pyrazolo[3,4-b]pyridin-5-yl)furan-2-yl)acrylamide (**36**)</u>
Yield: 8 mg (51%). ^{1}H NMR (400 MHz, DMSO) δ 9.07 (d, 1H, J = 2.1 Hz), 8.68 (d, 1H, J = 2.1 Hz), 8.01 (s, 1H), 7.46 (d, 1H, J = 3.7 Hz), 7.43 (d, 1H, J = 3.7 Hz), 2.53 (s, 3H); ^{13}C NMR (125 MHz, DMSO) δ 162.72, 156.52, 152.04, 147.50, 145.98, 142.03, 135.04, 126.51, 124.54, 117.84, 117.14, 113.91, 109.09, 100.04, 12.08; LRMS (ESI) Exact Mass: 293.09, Found: 294.4 ($M + H^+$).

<u>3-(3-(2-aminoquinazolin-7-yl)phenyl)-2-cyanoacrylamide (**37**)</u>
Yield: 36 mg (65%). ^{1}H NMR (400 MHz, DMSO) δ 9.15 (s, 1H), 8.37 (s, 1H), 8.31 (s, 1H), 8.03-7.90 (m, 4H), 7.82 (br s, 1H), 7.74-7.69 (m, 2H), 7.57 (dd, 1H, J = 1.6, 8.3 Hz), 6.93 (br s, 2H); ^{13}C NMR (125 MHz, DMSO) δ 162.61, 162.18, 161.23, 152.21, 150.55, 144.34, 140.24, 132.73, 130.89, 130.04, 129.79, 128.77, 128.54, 122.13, 120.92, 118.87, 116.54, 107.40; LRMS (ESI) Exact Mass: 315.11, Found: 316.1 ($M + H^+$).

<u>3-(3-(5-amino-1H-pyrazol-3-yl)phenyl)-2-cyanoacrylamide (**38**)</u>
Yield: 0.5 mg (1% over 2 steps). ^{1}H NMR (400 MHz, DMSO-d6): 8.18 (m, 1H), 7.91 (m, 1H), 7.83 (d, J = 8.0 Hz, 1H), 7.76 (app. t, J = 8.3 Hz, 1H), 7.64 (m, 3H), 7.55 (m, 2H), 7.30 (m, 3H); ESI-MS: 254.17(MH^+). Due to low yield there was not enough compound to characterize ^{13}C spectrum.

<u>(E)-2-cyano-3-[3-(6-oxo-1,6-dihydropyridin-2-yl)phenyl]acrylamide (**39**)</u>
Yield: 14 mg (35%). ^{1}H NMR (400 MHz, DMSO-d6): 8.32 (bs, 1H), 8.26 (s, 1H), 8.03–7.96 (m, 4H), 7.82 (bs, 1H), 7.68 (m, 2H), 7.61 (m, 1H), 6.47 (m, 1H); ^{13}C NMR (100 MHz, DMSO-d6): 163.3, 162.4, 158.6, 150.2, 147.9, 140.8, 135.8, 132.4, 130.3, 130.1, 129.6, 128.7, 116.3, 107.5, 106.7; ESI-MS: 266.18 (MH^+).

3-(3-(1,6-naphthyridin-8-yl)phenyl)-2-cyanoacrylamide (**40**)
Yield: 69 mg (92%). ^{1}H NMR (400 MHz, DMSO) δ 9.47 (s, 1H), 9.17 (dd, 1H, J = 1.8, 4.2 Hz), 8.84 (s, 1H), 8.70 (dd, 1H, J = 1.8, 8.2 Hz), 8.34-8.31 (m, 1H), 8.29 (s, 1H), 8.06-7.93 (m, 3H), 7.82-7.77 (m, 2H), 7.76-7.70 (m, 1H); ^{13}C NMR (125 MHz, DMSO) δ 163.04, 155.52, 153.65, 150.78, 147.28, 146.12, 136.77, 136.57, 134.79, 132.26, 132.06, 131.98, 129.56, 129.26, 123.52, 123.49, 116.61, 107.19; LRMS (ESI) Exact Mass: 300.10, Found: 301.34 (M + H^+).

3-(5-(1,6-naphthyridin-8-yl)furan-2-yl)-2-cyanoacrylamide (**41**)
Yield: 50 mg (quant.). ^{1}H NMR (400 MHz, DMSO) δ 9.45 (s, 1H), 9.38 (s, 1H), 9.30 (dd, 1H, J = 1.7, 4.3 Hz), 8.71 (dd, 1H, J = 1.7, 8.2 Hz), 8.13 (d, 1H, J = 3.7 Hz), 8.09 (s, 1H), 7.86 (dd, 1H, J = 4.3, 8.2 Hz), 7.53 (d, 1H, J = 3.7 Hz); ^{13}C NMR (125 MHz, DMSO) δ 162.56, 155.56, 153.96, 153.02, 147.70, 145.41, 143.78, 137.02, 135.16, 124.21, 123.68, 123.09, 120.17, 117.62, 116.96, 101.47; LRMS (ESI) Exact Mass: 290.08, Found: 291.1 (M + H^+).

(E)-2-cyano-3-[1-(6-methylpyrazin-2-yl)piperidin-4-yl]acrylamide (**42**)
Yield: 8.7 mg (7%). ^{1}H NMR (400 MHz, CD_3OD): 7.98 (s, 1H), 7.64 (s, 1H), 7.34 (d, J = 10.0Hz, 1H), 4.58 (bs, 2H), 4.46 (m, 2H), 3.07–2.85 (m, 3H), 2.36 (s, 3H), 1.85 (m, 2H), 1.60 (m, 2H); ^{13}C NMR (125 MHz, DMSO-d6): 162.2, 160.2, 153.8, 150.1, 131.4, 128.2, 114.9, 111.4, 43.0, 29.2, 21.3; ESI-MS: 272.22(MH^+).

References

1. Irwin, J.J., Sterling, T., Mysinger, M.M., Bolstad, E.S. & Coleman, R.G. ZINC: A Free Tool to Discover Chemistry for Biology. *J Chem Inf Model* (2012).
2. Pilot, P. version 6.1; SciTegic Inc.: San Diego, CA 92123-1365.
3. Ouyang, X. et al. CovalentDock: automated covalent docking with parameterized covalent linkage energy estimation and molecular geometry constraints. *J Comput Chem* **34**, 326-36 (2013).
4. Mysinger, M.M. & Shoichet, B.K. Rapid context-dependent ligand desolvation in molecular docking. *J Chem Inf Model* **50**, 1561-73 (2010).